Shaking table test of seismic control system using tuned mass viscous damper with force restriction mechanism

M. Ikenaga
Tohoku University, Japan

K. Ikago & N. Inoue
Tohoku University, Japan

15 WCEE
LISBOA 2012

SUMMARY:
The force restriction of a tuned mass viscous damper is considered by using a rotary friction mechanism. From a series of shaking table tests, it is shown that the force-restriction mechanism can effectively limit the maximum damping force without deterioration of the maximum displacement of the primary system. The analytical results show good agreement with the experimental results, and the relationship between the restricted/unrestricted force ratio and the maximum displacement is examined by analyses.

Keywords: Seismic control structure, Tuned mass viscous damper, Shaking table test, Force restriction

1. INTRODUCTION

A dynamic vibration absorber (DVA), or a tuned mass damper (TMD), is a vibration control system that adds a secondary vibration system with damping to the primary system. Figure 1 shows the analytical model of a 1-degree-of-freedom (1-DOF) structure combined with a TMD. TMDs are considered to be effective against wind-induced vibrations, but not against earthquake-induced vibrations. Saito *et al.* (2008) thus developed a new type of TMD that is effective against earthquake-induced vibrations, and referred to this as a tuned mass viscous damper (TMVD). A rotary viscous damper configured with a cylindrical flywheel and a viscous material enclosed between the external and internal cylinders (Figure 2) is connected to the primary system with a soft spring to construct a TMVD vibration control system. The inertial and damping forces of the rotary viscous damper in the rotational direction are amplified by a ball screw mechanism when they are translated into the translational direction. The inter-story motion of the primary system is amplified by the secondary vibration system to produce a large deformation in the damper.

Although a TMVD seismic control system is very effective, a concern is that the excessively large damping force generated by the TMVD may cause damage in the damper or to the primary structure. To restrict the maximum damping force, the authors propose two force-restriction mechanisms. The first causes the supporting spring to yield and the second breaks the traction between the cylindrical flywheel and internal cylinder at a certain load. The mechanical model of this force-restriction mechanism is shown in Figure 3. The force restriction mechanism is connected in series between the supporting spring and MVD. Although analytical studies have examined the behavior of the force-restricted TMVD (FRTMVD) in previous studies, experiments have yet to be conducted. In this study, a FRTMVD is incorporated into the small-scale 1-DOF specimen, and the response characteristics of the FRTMVD seismic control system are examined by a shaking table test. Furthermore, the analytical results are compared with the experimental results to validate the analytical modeling and numerical analysis methods.

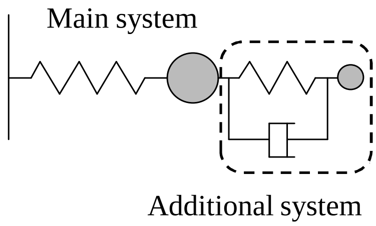

Figure 1.1. Dynamic vibration absorber

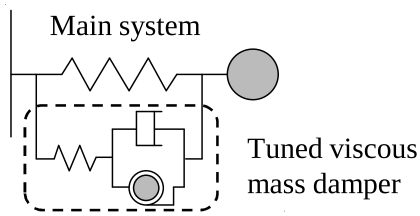

Figure 1.2. Tuned viscous mass damper

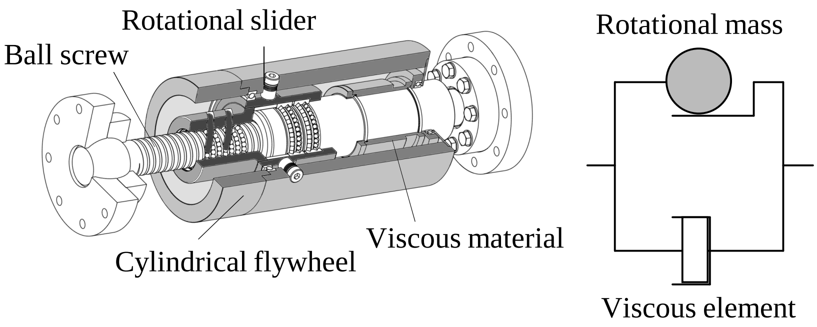

Figure 2 Viscous mass damper

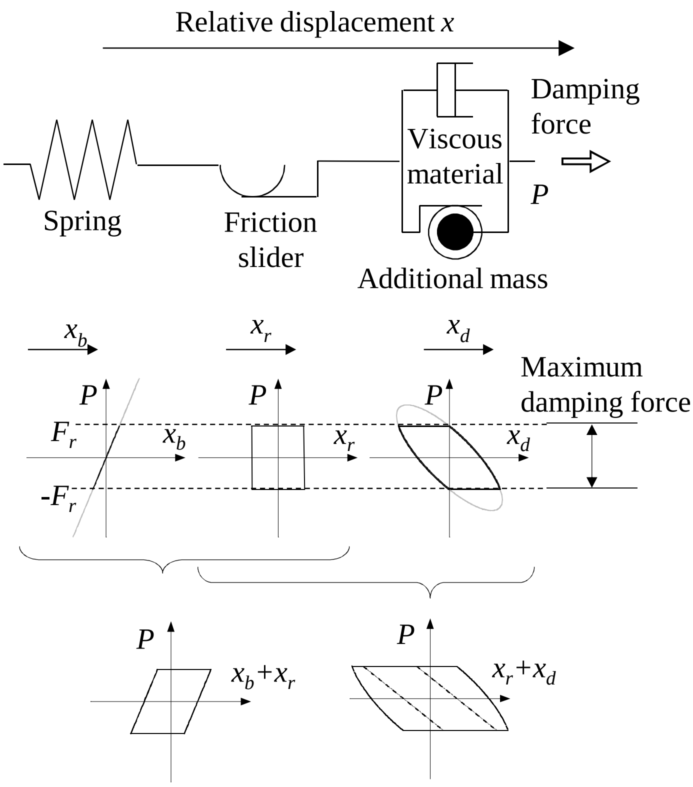

Figure 3 Force-restricted tuned viscous mass damper

2. MECHANISM OF FRTMVD

The analytical model of the FRTMVD is shown in Figure 3. x, x_b, x_r, and x_d are the relative displacement of the main frame, the deformation of the supporting spring, the slip displacement of the force-restricted mechanism, and the displacement of the MVD, respectively. F and F_r are the damping force and the restricted force of the damper, respectively.

The black and gray solid lines in Figure 3 represent the hysteresis of the FRTMVD and TMVD, respectively. The sum of displacements x_b, x_r, and x_d is the same as the displacement in the primary system x. In the case that the damping force is smaller than the limit force, the force-restriction mechanism remains inactivated and the slip displacement x_r remains zero. In the case that the damping force reaches the limit force, the damping force stops increasing and the slip displacement in the restriction mechanism x_r increases.

To realize the force-restriction mechanism, we consider two methods. One is to equip the rotary viscous damper with a rotary friction mechanism. When the force of the MVD becomes greater than the restriction force, rotational slip occurs in the friction material inserted between the ball screw nut and tubular flywheel. The analytical model of the FRTMVD using this mechanism is expressed as the combination of a friction slider and MVD. In this method, slip displacement in the force-restriction mechanism of the MVD occurs in the rotational direction so that residual displacement cannot occur in the translational direction.

The second method is to allow the supporting spring to yield at a certain limit load. Although a residual plastic displacement occurs in the supporting spring in this case, the damper behavior is same as that in the first method.

When the damping force is restricted, the dissipated energy in the MVD decreases compared with the force-unrestricted TMVD, but the hysteresis in force-restriction mechanism compensates for the loss of energy dissipation and the seismic control performance remains effective.

3. SHAKING TABLE TEST OF 1-DOF STRUCTURE COMBINED WITH FRTMVD

A series of shaking table tests are conducted to compare the behaviors of the FRTMVD and TMVD. Furthermore, numerical analyses are conducted to validate the analytical model and numerical method.

3.1. OVERVIEW OF THE SPECIMEN

Figure 4 shows an elevated view of the small-scale 1-DOF specimen. Table 1 lists the specifications of the specimen and damper obtained from a preliminary static loading test and free vibration test. In this experiment, the friction damper is used as the force-restriction mechanism.

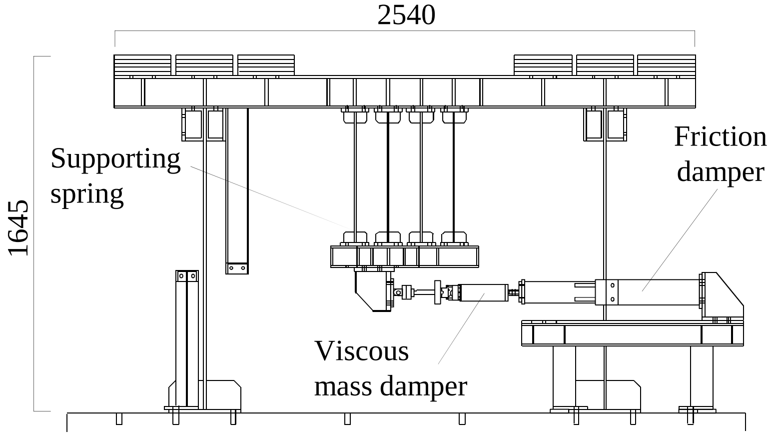

Figure 4. Elevated view of the specimen (unit:mm)

Table 1. Analysis parameter values

m	mass	t	2.1
k	stiffness	kN/m	268.0
c	damping coefficient	kNs/m	0.05
T	natural period	s	0.55
m_d	rotational mass	t	0.42
k_b	stifness of supporting spring	kN/m	77.4
c_d	damping coefficient of damper	kNs/m	2.0
F_d	internal friction of damper	kN	0.11

The north-south (NS) component of the Tohoku University record of the 1978 Miyagi-Oki earthquake (hereinafter termed the “Tohoku record”) and the NS component of the Japan Meteorological Agency, Kobe record of the 1995 Hyogo-ken Nanbu earthquake (hereinafter termed the “Kobe record”) are used as the input ground motions in the shaking table tests. The amplitudes of the input ground motions are scaled to 35% of the Tohoku record and 10% of the Kobe record, so that the specimen remains elastic.

Accelerometers are used to measure the acceleration on the shaking table and at the top of the specimen. A load cell is used to measure the damping force. Laser displacement transducers are used to measure the relative story displacement, displacement of the supporting member, and slip displacement of the friction damper, respectively.

The maximum force of the FRTMVD is considered as the experimental parameter. The maximum damping force of the FRTMVD is normalized by using the ratio between the restricted damping force and the unrestricted damping force. In the shaking table tests, the 1-DOF system with TMVD (hereinafter termed the TMVD model) and the 1- with FRTMVD (hereinafter termed the FRTMVD model) are considered. The restricted/unrestricted damping force ratio for the FRTMVD (hereinafter termed the “restriction ratio”) is determined as 0.6.

3.2. EXPERIMENTAL RESULTS

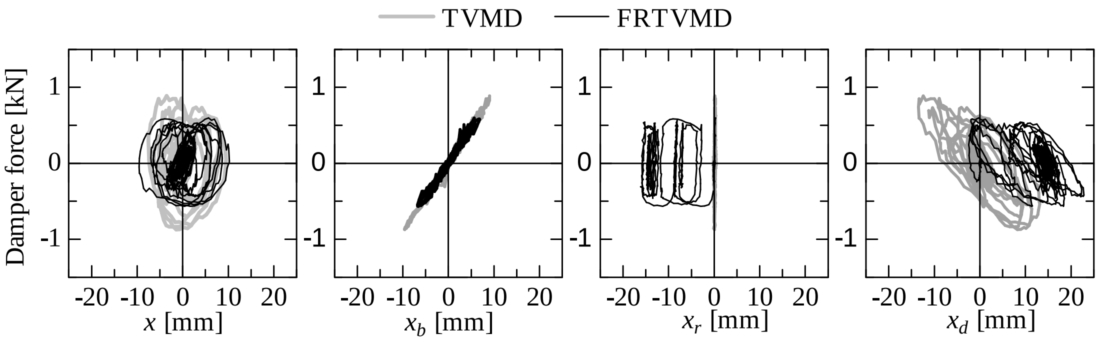

Figure 5-1. Comparison between TVMD and FRTVMD for the Kobe record

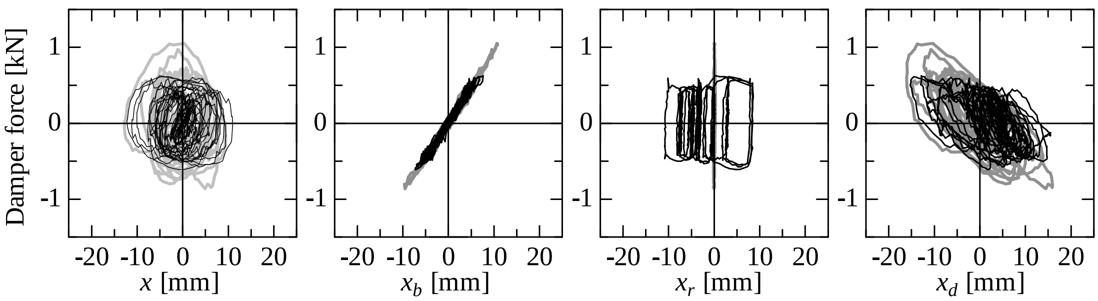

Figure 5-2. Comparison between TVMD and FRTVMD for the Tohoku record

Figure 5 shows the test results of the TMVD and FRTMVD models. The maximum relative displacement of the FRTMVD model and that of the TMVD model are almost the same for both ground motions. On the other hand, the maximum damping force of the FRTMVD model is reduced to 67% of that of the TMVD model in the case of the Kobe record, and to 59% of that of the TMVD model in the case of the Tohoku record. The response restriction ratio is almost the same as that determined in the previous section (0.6).
Figure 6 shows the test results of the energy responses. In the case of the TMVD model, only the MVD dissipates the energy. On the other hand, in the case of the FRTMVD model, the energy dissipation in the MVD decreases, but the friction damper dissipates energy such that the total energy dissipation is the same as in the TMVD model.

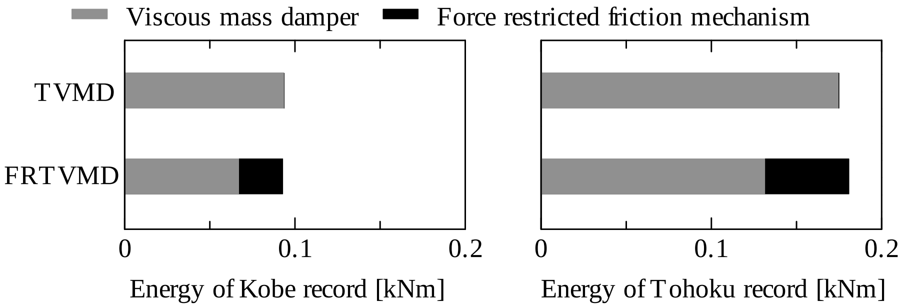

Figure 6 Energy dissipation

3.3. COMPARISON BETWEEN EXPERIMENTAL AND ANALYSIS RESULTS

A series of numerical simulations are conducted and the analysis results are compared with the experimental results to examine the validity of the analytical methods. Figure 7 shows the analytical model. The analysis parameter values are listed in Table 1. The acceleration measured in the shaking table tests is used as the input ground motion in this numerical study.

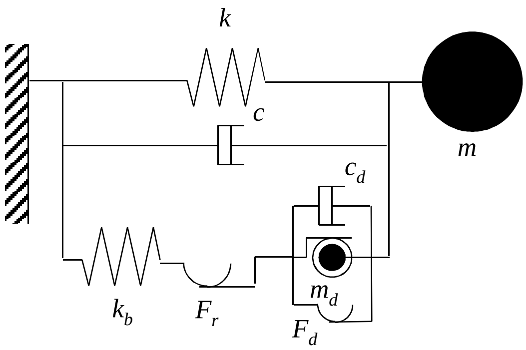

Figure 7. Numerical simulation model

Figure 8 shows a comparison between the experimental and analysis results. The relative displacement and the acceleration at the top of the frame obtained by both methods are almost identical. As shown in the hysteresis loops, it is obvious that the analytical displacements coincide well with the experimental ones for the Kobe record. In the case of the Tohoku record, the relative displacements show good agreement, but the displacements of the MVD and the friction damper are different from each other. This is because the slip displacement in the friction damper is difficult to simulate by the numerical method.

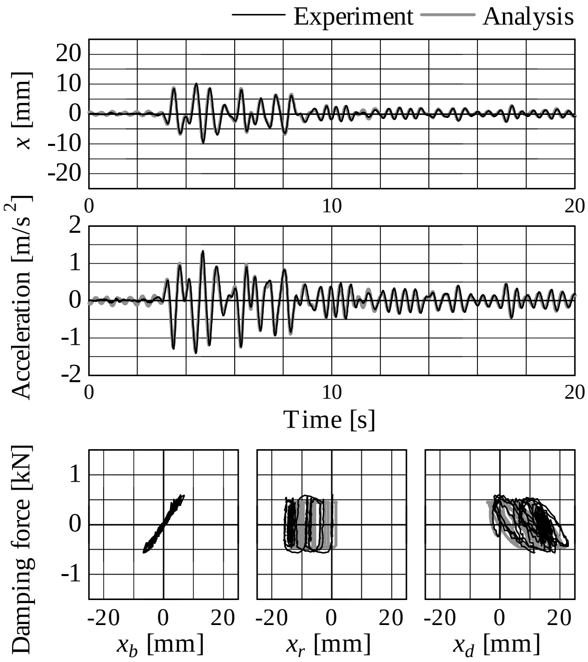

Figure 8-1. Comparison of Kobe record

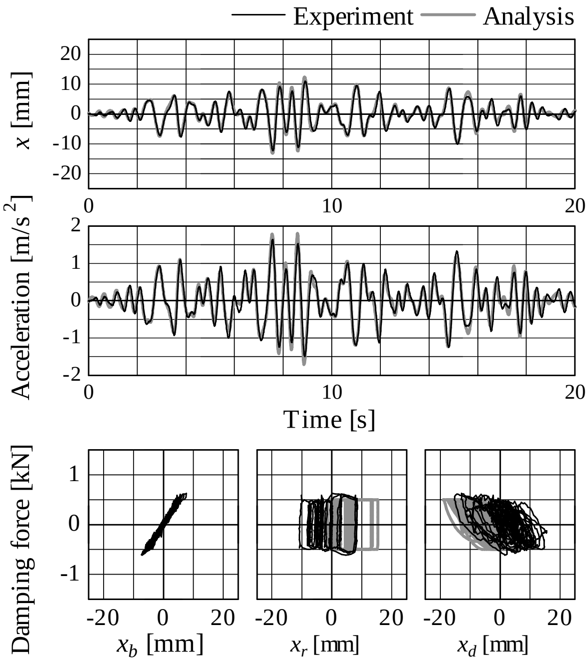

Figure 8-2. Comparison of Tohoku record

Figure 9 shows a comparison between the experimental and analytical energy dissipations. As mentioned above, the experimental and analytical results are different in terms of the slip displacement of the friction damper. But the hysteresis loops for the displacement and damping force are almost the same in both cases. This means that the energy dissipation in the experiment and analysis are almost the same.

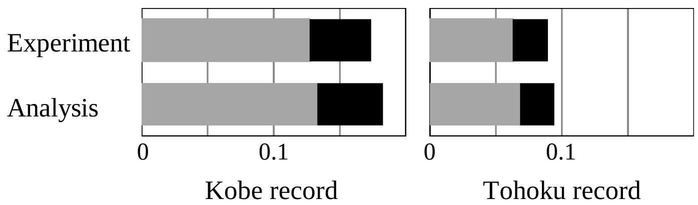

Figure 9. Comparison of energy dissipation

4. EFFECT OF FORCE RESTRICTION AND ITS SCOPE OF APPLICATION

As shown above, it is clear that the numerical analysis can accurately simulate the behavior of the 1-DOF system with the FRTMVD. In this section, by using the numerical simulation, the relationship between the restriction ratio and maximum relative displacement is considered.

4.1 OVERVIEW OF ANALYSIS

The analytical model and parameter values used in this section are shown Figure 7 and Table 1, respectively. Parametric studies are conducted by varying the restriction ratio from 0.1 to 1.0 at 0.01 intervals. The acceleration measured in the shaking table tests, the Tohoku record scaled by 35%, and the Kobe record scaled by 10% are used as the input ground motions.

4.2 PARAMETRIC ANALYSIS RESULTS

Figure 10 shows the relationship between the restriction ratio and the maximum relative displacement.

The maximum relative displacement is almost unchanged when the restriction ratio is increased from 0.5 to 1.0 in the case of the Kobe record and from 0.6 to 1.0 in the case of the Tohoku record. In these restriction ratio ranges, the FRTMVD can maintain the maximum relative displacement of the TMVD but with a smaller damping force. When the restriction ratio is outside of these ranges, the maximum relative displacement increases and the effect of the FRTMVD damper deteriorates.

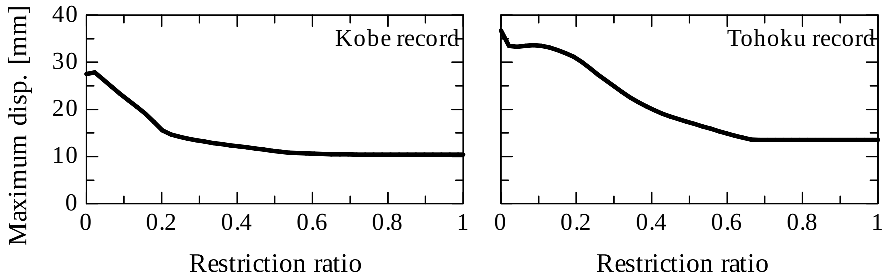

Figure 10. Relationship between restriction ratio and maximum displacement

Figure 11 shows the time profiles of the displacements when the restriction ratio is 1.0, 0.6, and 0.1. In the case that the restriction ratio is 1.0, the displacement of the supporting spring and the displacement of the MVD are out of phase by approximately half of a wavelength, and the slip displacement of the friction damper remains at 0. In the case that the ratio is 0.6, slip displacement of the friction damper occurs, and the displacement of the MVD is shifted in response to the displacement of the friction damper. But the displacement of the MVD and the displacement of the supporting spring are out of phase by approximately half of a wavelength, so that the characteristics of the TMVD are preserved.
In the case that the restriction ratio is 0.1, the displacement of the MVD and the displacement of the supporting spring become very small, and the displacement of the friction damper increases substantially. The relative displacement is almost the same as the slip displacement of the friction damper, and the relative displacement becomes larger than the displacement of TMVD. Thus, in the case that the restriction ratio is very small, the displacement of the MVD and the slip displacement in the supporting member become very small, and then the damping performance of the FRTMVD can no longer be preserved.

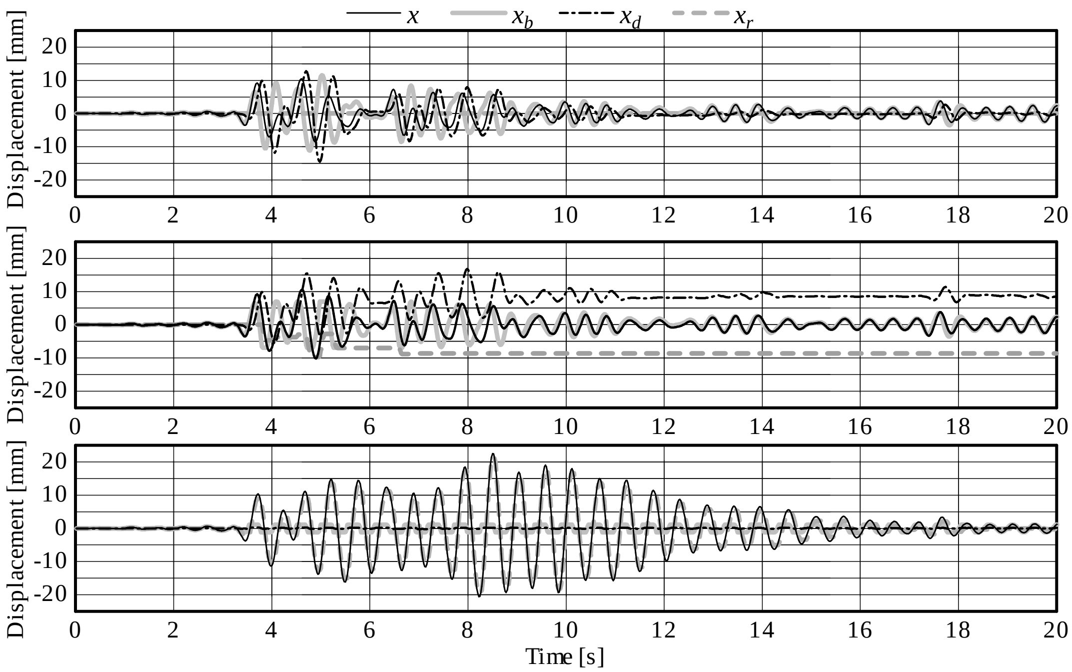

Figure 11. Displacement and force restriction

5. CONCLUSION

The advantages of the FRTMVD are considered from shaking table tests using a 1-DOF specimen combined with the FRTMVD. The shaking table test results show that the FRTMVD with a restriction ratio 0.6 can retain the damping performance of the force-unrestricted TMVD, and can reduce the damping force. Furthermore, from a comparison between the experimental results and the analysis results, it is shown that the relative displacement and the damper force can be evaluated with high accuracy.

By conducting a parametric analysis, the relationship between the relative displacement and the restriction ratio is considered. The results show that the damping performance of the FRTMVD with a restriction ratio of 0.6 is almost same as that of the TMVD.

REFERENCES

J.P.Den Hartog. (1985). Mechanical Vibrations, 4thed., Dover, New York

Saito, K., Kurita, S. and Inoue, N. (2007). Optimum response control of 1-DOD system using linear viscous damper with intertial mass and its kelvin-type modeling, Journal of Structural Engineering, Vol.53B, 53-66.

Saito, K., and Inoue, N. (2007). Optimum response control of 1-DOD system using linear viscous damper with intertial mass and its kelvin-type modeling, Journal of Structural Engineering, Vol.53B, 53-66.

Saito, K., and Inoue, N. (2007). A study on optimum response control of passive control systems using viscous damper with inertial mass, substituting equivalent nonlinear viscous elements for linear viscous elements in optimum control systems, AIJ J. Technol. Des. Vol 13, No.26, 457-462.

K. Saito, Y. Sugimura, S. Nakaminami, H. Kida and N. Inoue: Vibration Test of 1-story Response Control System Using Inertial Mass and Optimized Softy Spring and Viscous Element, Proceedings of the 14th World Conference on Earthquake Engineering, CD-ROM paper ID:12-01-0128, 2008.10.

Saito, K., Nakaminami, S., Kida, H., and Inoue, N. (2008), Vibration tests of 1-story response control system using intertial mass and optimized softy spring and viscous element, Journal of Structural Engineering, Vol.54B, 623-634.

Saito, K., Sugimura, Y., Ikago, K., and Inoue, N. (2008), A study on response control of a structure using viscous damper with inertial mass, Journal of Structural Engineering, Vol.54B, 635-648.

Sumiyama, T., Arai, T., Ikenaga, M., Ikago, K., and Inoue, N. (2010), A study on a seismic vibration control system using a tuned viscous mass damper : Part1-2, Proceedings of AIJ annual conference, B-2, 449-450.

Isoda, K., Hanzawa, T., Fukasawa, T., and Fukukita, A. (2010), Development of Inertia Mass Damper with Overload Prevention Function : Part 1. Purpose of Development and Summary of the Damper, Proceedings of AIJ annual conference, B-2, 453-454.